Andreu Bonet Navarro

BONDING PDMS TO OTHER MATERIALS FOR FUTURE OPTICAL-BASED MICROFLUIDIC DEVICES

MASTER'S DEGREE THESIS

supervised by Dr Jaume Massons

MASTER'S DEGREE IN NANOSCIENCE, MATERIALS AND PROCESSES

UNIVERSITAT ROVIRA I VIRGILI

Tarragona

2018

Bonding PDMS to other Materials for Future Optical-Based Microfluidic Devices

Andreu Bonet Navarro
Master Program in Nanoscience, Materials and Processes, 2017-2018
e-mail: andreu.bonet@estudiants.urv.cat

Supervisors: Jaume Massons.
Department of Physical and Inorganic Chemistry. Universitat Rovira i Virgili
Campus Sescelades, c/. Marcel·lí Domingo, s/n Tarragona, 43007, Spain.

Abstract: Microfluidics is a research field that is gaining a lot of attention in recent years, due to the reduced costs and increased efficiency of all the instrumentation based on this technology, including optical-based one. Due to that, the necessity to bond interesting optical materials, such as $KLu(WO_4)_2$ crystals in our case, to the most commonly used materials in microfluidics, like PDMS and glass, to produce optical-based microfluidic devices, is increasing as well. In this work, different strategies to bond PDMS to PDMS and PDMS to glass will be optimized and compared with two of the most used direct bonding techniques such as oxygen plasma treatment and partial curing of PDMS. In addition, oxygen plasma treatment will be adapted to bond PDMS to $KLu(WO_4)_2$ in order to fabricate optical-based microfluidic devices. Moreover, mechanical properties of Sylgard 184 PDMS from Dowsil such as Young Modulus and Ultimate Tensile Stress will be studied to clarify the reported bibliography based on PDMS.

INTRODUCTION

Nowadays microfluidics is becoming an interesting research field in a lot of disciplines, but mostly in chemical engineering[1], biotechnology, biomedicine[2,3] and analytical chemistry[4], because it helps to decrease the size of the liquid-gas based instrumentation, allowing the integration of multiple subunits and functions in a single device reducing its costs. In addition the reduced amount of the reagents needed for the microfluidic devices makes possible to control the temperature and the reagents concentration faster and more precisely[5].

Polydimethylsiloxane or also called PDMS is one of the most used materials in microfluidics due to its extraordinary properties[6], like the possibility to mould features at nanoscale resolution (>10nm) with relatively low shrinkage (around 1%), high elasticity, non-toxicity, transparency in the visible spectrum and low cost, making this material very attractive in this area[7]. In addition this material it's very easy to fabricate and manipulate, because to produce it we only need to mix a high viscosity prepolymer with its curing agent at relatively low temperatures[8] (from 25°C to 200°C) to initiate the thermal curing obtaining the final solid elastomer[9]. In addition, photocurable PDMS have been reported[10] as well.

PDMS is formed by two precursors: the curing agent (or also called crosslinker) and an elastomer. The curing agent is composed of a dimethylsiloxane polymer, a siloxane crosslinker and an inhibitor, while the elastomer component consists on dimethylsiloxane polymer, reinforcing silica and platinum catalyst[11]. By mixing the prepolymer and the curing agent in a 10:1 weight ratio we obtain the final product with, in general, the most promising mechanical characteristics. Also, different ratios can be used to obtain different properties. The final product **(figure 1)** consists on an alternated polymer backbone made of silicon and oxygen atoms with methyl groups attached to them forming long chains[12].

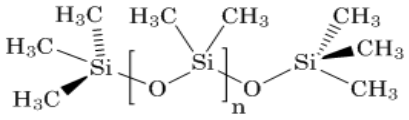

Figure 1: Chemical structure of PDMS.

Due to the interesting physical-mechanical[13], optical[14,13] and surface[15,13] properties of PDMS his applications are in fact quite extended, such as protective coatings[16], solar concentrators[17,18] waveguides[19] microfluidic channels[20,21], microvalves[22,] and micro membranes[23]. For the use of PDMS in microfluidic devices sometimes we need to bond this material to another material, in an indirect or direct way to form the final microfluidic device. Indirect bonding means that an adhesive or intermediate layer between the bonded materials is used, and direct bonding is whenever there isn't any extra substance between the two bonded surfaces. Normally indirect bonding is easier and more simple to achieve but it's not a "clean bond" because another material, that acts as adhesive layer[24], is embedded between the two bonded substrates and can interfere in the properties of the final device. Direct bonding techniques despite its complexity to manage, can give more clean, high quality and stronger bonds than indirect methods[25], therefore they are preferable over indirect ones when high quality devices are desired.

In recent years, $KLu(WO_4)_2$ (or also called KLuW) crystals are starting to be studied in consequence of its interesting optical properties as a laser host[26,27]. Due to that, the integration of KLuW crystals, acting as optical active material in PDMS made microfluidic circuits, is becoming one of the future goals in our research group, to produce optical-based microfluidic devices[28], reducing the size and increasing the efficiency of the current ones. We will also work with glass to overcome some of the limitations of PDMS, like lower aspect ratios of its microstructures (normally 20:1 for glass[29] and 10:1 for PDMS[30]), including higher insulating properties of glass compared to PDMS, that are interesting to design microfluidics circuits[31].

Partial curing of PDMS is one of the most relevant direct bonding techniques to bond PDMS to PDMS (from now on PDMS/PDMS) surfaces[25]. This technique consists on attaching two partially cured PDMS substrates solid enough to be demoulded. The remaining active chains of the partially cured prepolymer will mix and react with the active chains of the other layer producing a bond between them, joining the two PDMS layers[25]. Therefore, as less cured the PDMS layers are, stronger will be the bond, because more polymer chains will form a bond between the two layers. Considering this fact, the strongest bonds are expected to be found at low curing times or when the curing rate is as low as possible, but the polymer is already solid enough to retain the features and not fail during demoulding. In one hand, partial curing presents a lot of advantages in terms of simplicity and low costs because only a low temperature furnace is required[32]. Also, a simple surface cleaning of the moulds used for the PDMS manufacture, involving acetone and compressed air, is enough. In the other hand, we need to consider that since this method involves the partial curing of PDMS into moulds, the optimal curing time can change from one specific mould to another, depending on the size, shape and nature of it. These factors strongly affect the heat transfer, modifying the time needed to reach the minimum temperature required to start the curing process[8]. Due to that fact, and the possibility to bond only PDMS/PDMS surfaces, partial curing bonding is not a quite versatile technique. Oxygen plasma is another relevant direct bonding method to bond PDMS surfaces, not only to another PDMS surface, but also to any material whose surface is activable by this plasma[12]. Both PDMS and glass surfaces can be easily activated by oxygen plasma, so either PDMS/PDMS and PDMS to glass (from now on PDMS/glass) bonding can be performed by this method. The chemical composition of PDMS **(figure 1)** and glass surfaces is quite similar, with main compositions of Silicon (Si) and Oxygen (O) atoms forming Si-O bonds as can be seen on **figure 2**. Both surfaces are activated through the substitution of one of the four Si bonds by an hydroxyl (-OH) group under oxygen plasma conditions[12] as represented in step 1 of **figure 2**. After the activation of both surfaces, they are attached together putting them under physical contact to produce the "bonding reaction" between (-OH) on both layers. The reaction takes place producing -Si-O-Si- bonds where one Si atom belongs to one surface and the other belongs to the other surface. After that, both surfaces are bonded chemically, as can be seen in step 2. Contrary to partial curing, oxygen plasma is an extremely versatile technique that can bond so many different types of sample with different surfaces, shapes and compositions; but is more expensive and complex to perform because RIE instrumentation and cleanroom facilities[33] are needed. It's also important to note that the (-OH) groups formed during oxygen plasma treatment can change the nature the surfaces, making them more hydrophilic, which can be advantageous or disadvantageous depending on the applications of the device.

During the bibliographical research, some studies about two of the previously described bonding methods can be found, including its efficiency to bond PDMS/PDMS and PDMS/glass either with oxygen plasma[34] and partial curing (only for PDMS/PDMS)[25]. However, due to the relevance of the lab conditions, mould nature and shapes commented before, we will perform experiments to adapt them to our lab conditions and future necessities. In addition, since in future studies we want to create an optical-based analytical device using a KLuW crystal[26,35] as the waveguide, and PDMS to create the microfluidic circuit, we need to find a way to join these materials together, but there isn't any reported methodology to bond KLuW to PDMS (from now on PDMS/KLuW) surfaces. In our laboratories, previous tests with oxygen plasma bonding were performed in order to bond KLuW/PDMS, because the oxygen atoms onto the KLuW surface[35], can be activated in a similar way than the ones present in Silicon Oxide based substrates. However, the obtained bond strength was extremely weak, and to obtain stronger bonds, a nanometric layer of SiO_2 had to be deposited onto the surface of KLuW, bonding them with an indirect way. But the deposited SiO_2 layer between the bonded materials could alter the optical properties of the final device. Then we decided to keep searching a way to obtain stronger bonds using oxygen plasma treatment. Our first explanation for this low bond strength obtained in previous experiments, is the relatively low flatness and non-proper cleaning process of the crystals surfaces before oxygen plasma treatment. Therefore, our task was to optimize the previous cleaning process. Furthermore, we will use polished surfaces to maximize the contact area between these two materials. Because since to produce the bonding reaction the surfaces must be in physical contact, as flatter are the surfaces, larger is the area in contact between them, and larger is the final bonded area, increasing the total bond strength between the surfaces[36].

Having said all of this, in this study we will try to perform and optimize two direct bonding methods, like partial curing of PDMS and oxygen plasma treatment, to bond between each other the tree previously described materials: PDMS(Sylgard 184 from Dowsil), KLuW and glass. In concrete, the following four bonding combinations of materials will be studied: PDMS/PDMS surfaces using PDMS partial curing method, PDMS/PDMS surfaces using oxygen plasma treatment, PDMS/glass surfaces using oxygen plasma treatment and PDMS/KLuW surfaces using oxygen plasma treatment, leaving the remaining combinations for future studies. In addition, mechanical properties like Young Modulus and Ultimate Tensile Stress of PDMS (Sylgard 184 from Dowsil) will be analysed and compared with the published data[8,37]. We expect that the information obtained in this study, like the bond strength between different materials widely used in microfluidics, and the studied mechanical properties of PDMS, will be useful for the future manufacture and design of optical-based microfluidic devices.

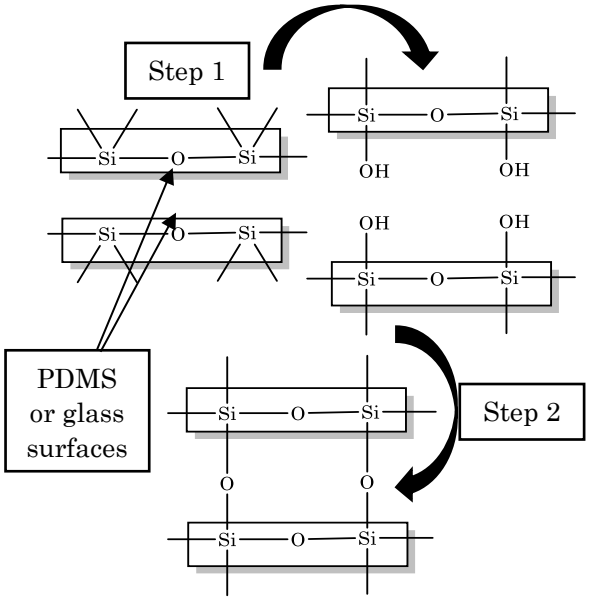

Figure 2: Scheme of the bonding procedure to bond either PDMS to PDMS and PDMS to glass using oxygen plasma treatment. The step 1 shows the surface activation of two surfaces under oxygen plasma conditions, and the step 2 represents the chemical bonding of the surfaces during physical contact.

EXPERIMENTAL SECTION

Bonding PDMS/PDMS with partial curing

The PDMS layers that will be used for partial curing bonding experiments were fabricated using glass moulds, manufactured using conventional glass slides, because their low cost and relatively flat surfaces makes them suitable to mould the PDMS layers for this bonding technique. These moulds consist on 4mm thick glass slides on the bottom/top, and two 1mm thick glass slides on the sides to ensure a uniform cavity with dimensions (27x40x1mm), to mould the PDMS layers, leaving front and back openings to facilitate the posterior demoulding. The PDMS layers were 1mm thick, because samples with different thicknesses generate problems during the posterior peeling tests (explained in more detail in the following sections).

After the manufacture and cleaning of the moulds with acetone and compressed air, we prepare around 20g of PDMS (Sylgard 184 from Dowsil) by mixing vigorously the prepolymer with the crosslinker at 1:10 ratio, in a 50ml beaker. After that, the mixture is degasified under vacuum, at least during 30 min or until trapped air bubbles disappear. The prepolymer mixture is moulded using the glass moulds previously described, first putting the mixture onto the bottom cover then sealing it with the top and side covers. Eleven glass moulds with the uncured mixture are put on a low temperature furnace at 65ºC until the prepolymer is solid enough to be demoulded without failure. We will call this time the optimal curing time because it's the moment at which we expect to obtain the strongest bonds, as commented previously in the introduction. To find that time in each experiment, we periodically take out of the furnace only one of the moulds every 1 min, to check if it can be already properly demoulded or collapses. When we reach that time, the rest of ten moulds are taken out of the furnace in couples every 2 min during around 10 minutes, to study the effect of curing time in the bond strength, and then waiting for them to reach the room temperature before demoulding. The partially cured PDMS layers are attached together in couples. At the same time, we place 1Kg flat object onto the samples, to apply a homogeneous pressure on them, ensuring uniform surface contact, to guarantee homogeneous bonding. After that, they are placed again into the furnace at 65 degrees for at least 2h to complete the curing reaction, obtaining five samples bonded at different curing times. Before bonding the PDMS layers we place a layer of aluminium on one side between them, to avoid the bonding in this region **(figure 3)**, to facilitate the posterior peeling process. When the curing process is complete we take the samples out of the furnace and cut all of them with the same width (17mm) using a razor blade, to obtain comparable results in the bond strength tests. The same procedure is repeated under the same conditions, for two additional days to study the repeatability.

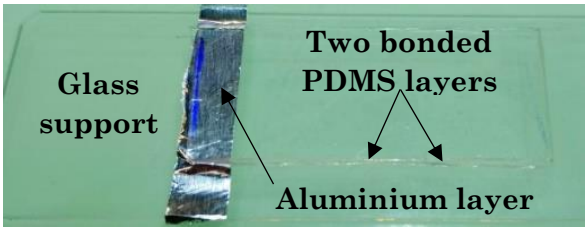

Figure 3: Image of two bonded PDMS layers using partial curing supported on glass. The aluminium layer is placed between the two PDMS layers to avoid the bonding in this region.

Bonding PDMS/PDMS with oxygen plasma

To perform PDMS/PDMS bonding tests with oxygen plasma, eighteen PDMS layers were fabricated using the same methodology and dimensions used for partial curing bonding, but in this case, they were placed on the furnace for 2h and 30min until they were completely cured. The final eighteen layers obtained were cut with the same dimensions than the ones used for partial curing, using a razor blade, to make them easily comparable with the previous.

For oxygen plasma treatment bonding, only six of the eighteen PDMS layers were bonded each day, during three consecutive days to study the repeatability of the procedure. Prior to oxygen plasma treatment, the PDMS layers were cleaned carefully using acetone and compressed nitrogen (N_2) in a cleanroom environment. The surface of the PDMS layers were activated with oxygen plasma generated using a Reactive Ion Etching (RIE) instrument (PlasmaPro 80 RIE from Oxford Instruments). After trying to optimize the data available in the bibliography[38] without success, the optimal bonding conditions of the plasma were found by trial and error procedure. These optimal conditions are: Power: 20W, Pressure: 80mTorr, Exposure time: 20", Oxygen flow: 50 sccm. After oxygen plasma treatment, the six PDMS layers were removed from the instrument chamber and attached together in couples, putting an aluminium layer **(figure 3)** between them, as in partial cure bonding, obtaining a total of three samples each day. At the same time, we placed 1Kg flat object onto the samples in the same way and reasons used in partial cure bonding. It's important to note that the surface of the PDMS layers can start deactivating after ten or fifteen seconds after exposing them under atmospheric conditions, so is critical to attach them under that time. Finally, nine samples with the same configuration represented in **figure 3** were obtained for bond strength analysis.

Bonding PDMS/glass with oxygen plasma

To execute PDMS/glass bonding, firstly nine PDMS layers were fabricated with the same dimensions and methods described in the previous sections, and nine cover slips were used as glass substrate. The cleaning process is the same as the one used for the oxygen plasma bonding experiments either for the PDMS layers and cover slips. Three PDMS layers and three cover slips were placed into the oxygen plasma chamber to activate its surfaces each day, during 3 different days, using the same plasma conditions described in the previous section. After that, both materials were joined together to perform the bonding, following the same procedure used for bonding PDMS/PDMS with oxygen plasma. The final nine bonded samples had similar aspect to the ones in **figure 3**, but in this case the glass is directly bonded to one PDMS layer, instead of acting like a support material.

Bonding PDMS/$KLu(WO_4)_2$ with oxygen plasma

To accomplish PDMS/KLuW bonding, three PDMS layers were prepared accordingly to the previously described methodologies and dimensions. The only available KLuW substrate during the realization of this study was one KLuW crystal, grown with top-seed solution-growth methodology[26]. The dimensions of the crystal were: 18x12x2 mm. The crystal was cut and polished parallel to the **b** crystallographic direction, with an average surface roughness of 6.76 nm. Before oxygen plasma treatment the crystal was cleaned carefully with the following procedure: 1-Acetone under ultrasonication (10 min) → 2-Etanol under ultrasonication (10 min) → 3-Deionized water under ultrasonication (10 min) → 4-Orthophosphoric acid under ultrasonication at 60°C (10 min) → 5-Deionized water under ultrasonication (10 min) → 6-Piranha (H_2OSO_4:H_2O_2) (2:1) under ultrasonication (10 min) → 7-Deionized water under ultrasonication (10 min); while the PMDS layers were cleaned following the same procedure used in PDMS/glass bonding. After the cleaning procedure, the KLuW crystal is placed into the oxygen plasma chamber along with one PDMS layer. The plasma conditions were the following: Power: 15W, Pressure: 35mTorr, Exposure time: 30", Oxygen flow: 50 sccm, which are the ones used in previously commented experiments. Note that, they are relatively not aggressive (low exposure time and low power), to avoid surface damage of the crystal[39], which low surface roughness is crucial to obtain a good bonding[36]. After oxygen plasma treatment the samples are removed from the oxygen plasma chamber and attached together to produce the bond, putting also a 1Kg flat object over them for the same reasons in the previous sections. The same procedure was repeated for the two remaining PDMS layers, on two different days, using the same KLuW crystal.

Peeling tests of PDMS/PDMS samples

The bond strength of PDMS/PDMS samples were analysed by T shape peeling tests, performed using a Lloyd-Ametek EZ50 Universal Testing Machine, either for partial curing and oxygen plasma bonded samples. The set-up of the experiments is represented in **figure 4**. The PDMS samples are hold by the grip zones, using the machine jaws, and the load needed to peel the samples is generated by extending the upper jaw at a constant rate of 5mm/min, which is slow enough to avoid premature collapses of the samples, while maintaining static the bottom one. During that process, a strong and focused stress is produced in a narrow zone, located in the edge among the peeled zone and non-peeled zone of the PDMS layers, which we call peeling stress zone **(figure 4)**. The load necessary to peel the sample in front of the machine extension is recorded using a 100N Load cell (0,1% error) and NEXYGEN Plus Materials Testing (edition 4) [Software]. (10-Oct-2017), for further data analysis.

The bond strength, obtained for T shape peeling tests depends mainly on two factors: the quality of the bond, and the area of the peeling stress zone. The quality of the bond is influenced by the bonding techniques used and how well optimized they are. While the area of the peeling stress zone is calculated multiplying his length, equal to the width of the bonded PDMS layers, and his amplitude, which depends on the different bending accommodations of the PDMS layers for different PDMS thicknesses and even for different stages of the peeling procedure. Because of that, all tested samples had the same width (17mm) and thickness (1mm) to easily compare the quality of the bond among the different bonding methods. Despite of the significant importance of the amplitude of the peeling stress zone, it's difficult to calculate or estimate its value. Then, since all the used samples had the same thickness we considered it as a constant value in all of them. Therefore, the bond strength measured, or also called "peeling stress" during T shape peeling tests, independent on the width of the sample, is calculated dividing the load necessary to peel the sample by the width of the PDMS layers.

There are two different cases of peelings: The ideal peeling, and the peeling of a permanent bonded sample. During an ideal peeling test **(figure 5)**, the load needed to peel the sample increases first somewhat linearly due to the elongation of the highly flexible PDMS, until the sample starts to be peeled. It's also important to note that in some cases the load don't starts at 0, and this is due to the initial accommodations between the sample and the machine jaws. When the sample is being peeled the load remains constant, but in most cases with small variations due to the non-uniform bond quality along the bonding interface, or little momentarily changes in the bending accommodations, that can make the area of the peeling zone vary, as commented before. The bond strength is equal to the average value of the load found in this peeling zone. When the samples are completely peeled-off or collapsed, the load decreases almost instantaneously, and after that, in most cases the load is stabilized similarly to the one shown in **figure 6**, but in some cases, it lasts a little bit more to stabilize, like in **figure 5**, because even after the complete peel of the samples they are still in physical contact, producing unexpected forces due to the friction and bending accommodations between the two peeled PDMS layers. In all tests, the final load is a little bit higher than 0 because of the weight of the PDMS layer hold by the upper jaw. Then to obtain the real peeling stress (N/m) values, first we discounted the average values of the load found in the final part of the graphs, which corresponds to the weight of the samples, to the average load found on the peeling zone divided by the width of the PDMS layers. Note that, the peeling stress is defined by Newtons per unit length (N/m) instead of per unit area (N/m^2), contrary to the actual definition of stress. Because as commented before the area of this zone is hardly to measure, in addition, since this zone is extremely narrow and presents no high variations from one experiment to another, we consider it just as straight line that only depends on the width of the peeled samples.

There are some cases in which we can't calculate quantitatively the peeling stress, because the PDMS layers collapses before starting to be peeled-off. This samples are called permanent bonded samples. A failed sample can be seen in **figure 7**. Also, on **figure 6** it's possible to see how the load decreases instantaneously before reaching the peeling stress zone, unlike in **figure 5**, which indicates that the bond itself is stronger than the PDMS layers leading to the failure of the samples before starting to be peeled-off.

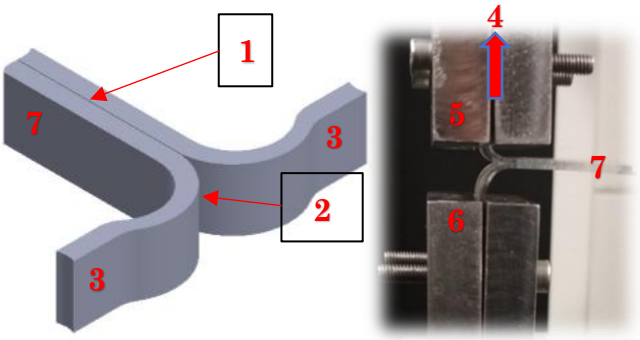

Figure 4: The illustration on the left is a schematic representation of PDMS to PDMS bonded samples used for the T shape peeling tests, whereas the image on the right, is a real photo of the tests set-up. The parts are signalled using numbers on the figure: 1-Bonding interface, 2-Peeling stress zone, 3-Grip zones, 4-Extension direction, 5-Upper Jaw, 6-Bottom jaw, 7-PDMS layers.

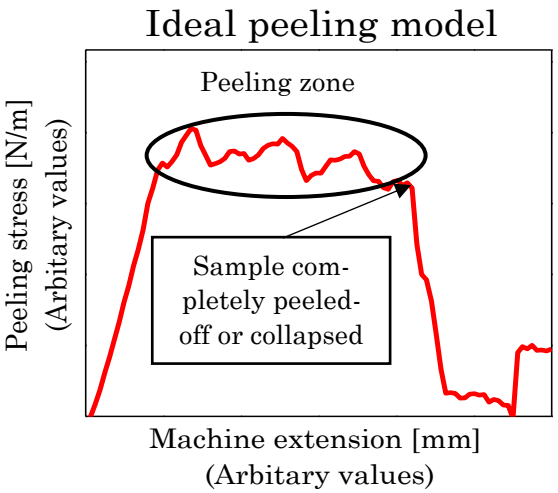

Figure 5: This graph represents a nearly ideal case of a T shape peeling test, where the load is represented in front of the machine extension.

Peeling tests of PDMS/glass samples

The peeling tests for samples that consists on a solid material, and an elastic one, can't be performed by T shape peeling, like in the previous section, because of the impossibility to bend the solid layer. Therefore, this sort of samples is normally peeled using 180° or 90° peeling tests. Since it is proved that the

peeling angle can affect the strength needed to peel them[40], we just performed 90° degrees peeling tests for all the PDMS/glass samples, described in the following paragraph, to obtain comparable results. Unfortunately, the 90° degrees peeling tests for PDMS/glass samples will give different results than the T shape peeling tests for PDMS/PDMS samples even when the same real bond strength is obtained.

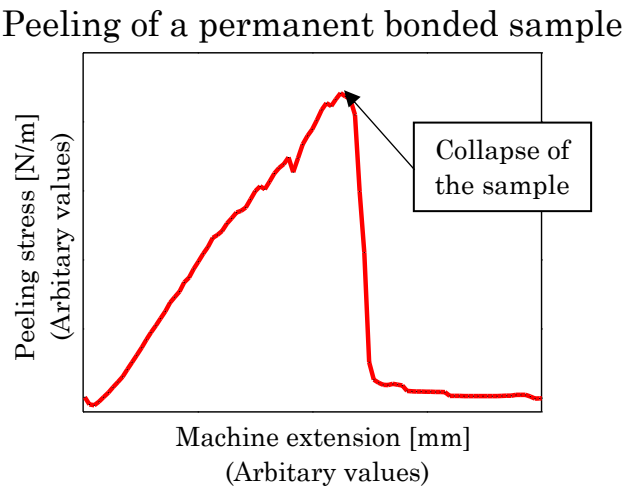

Figure 6: This graph is a peeling model of a permanent bonded sample in which the sample collapses before starting to be peeled. Where the load is represented in front of the machine extension

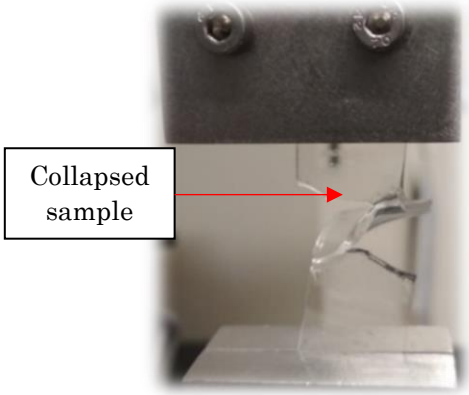

Figure 7: On this image its represented sample that collapses before starting to be peeled-off.

The set-up of the 90° peeling tests was like the previous T shape ones **(figure 8)**, where the flexible layer (the same PDMS layers used in the previous peelings) is hold by the upper jaw but, contrary to the T shape tests, a cover slip (solid glass layer) is just supported parallel to the surface of the bottom jaw. Moreover, as can be seen in **figure 8**, the extension direction of the upper jaw is perpendicular to the cover slip surface. Regarding to the conditions used on 90° peeling tests experiments, the same Universal testing machine, load cell and extension rate used in the previous peeling tests were applied. Furthermore, the data pretreatment, processing and analysis was identical to the previous described peeling tests.

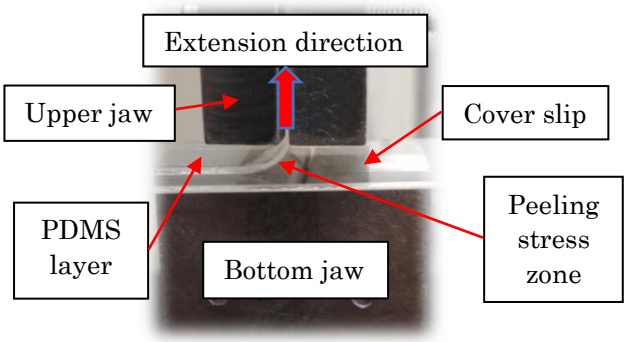

Figure 8: Set-up of the 90° peeling tests for PDMS/glass bonded samples. The extension direction of the upper jaws is shown using a thick red arrow while slim red arrows are used to show the rest of the parts.

Stress-strain tests for PDMS

Stress-strain tests were performed to calculate the Young Modulus and the Ultimate Tensile Stress for PDMS, using PDMS "dogbone" shape samples **(figure 9)**, commonly used for stress-strain tests[8,41], along with the same universal testing machine used for peeling tests. The PDMS samples were manufactured accordingly to the ASTM D412[42] models. The shape of these models allows us to obtain representative and good quality results, because the failure of the samples, and most of its elongation, always will be within the slimmer zone **(see figure 9)** that is the only part used to study the mechanical properties. In addition, the high width of the wider zone of the samples, makes them easy to grip by the jaws of the universal testing machine during stress-strain tests, and leads to low elongations of this part, making them negligible in samples with low elasticity. Despite of all these advantages, it's important to note that the elongation of the wider zone in highly elastic samples like PDMS, its always considerable, leading to false results, because the machine only records the total elongation of them, then a correction factor must be applied. The correction factor is calculated by theoretical simulations of the experiment using Comsol Multiphysics. After the simulation, the elongation of the slimmer zone is divided by total elongation of the samples (including the wider and slimmer zones), obtaining a correction factor of 0.48, which is pretty similar to values found in some previous simulations 0.5[37] and 0.4[8]. The shape of the samples during the simulation was the same than the real ones following the same ASTM D412 models. The Young Modulus and Poisson ratio were nearly realistic values which were the default values given by Comsol which are 0.750MPa and 0.49 respectively. It's important to note that no differences in the correction factor were found, when different or arbitrarily values for these parameters were selected.

The PDMS samples used in stress-strain tests were moulded using PMMA moulds. That moulds were obtained from cutting a 2mm thick PMMA slides, using a CO_2 laser, with the dimensions and shape shown on

figure 9, in order to mould 2mm thick PDMS samples, with the same dimensions. We selected a thickness of 2mm for that samples, because with lower thicknesses the samples started to show scratches during the final demoulding process, and for higher thicknesses the samples are not griped properly by the machine jaws of the universal testing machine during the stress-strain tests. Previously to stress-strain tests, twenty-seven PDMS samples were prepared, by filling twenty-seven PMMA moulds, with uncured PDMS (prepared with the same procedure described in the previous sections), then sealed with another two PMMA slides on the bottom and top of them, before putting them in the oven at 80°C for 2h to complete the curing process. Finally, the samples were taken out of the oven and removed from the moulds, cutting small layers of wasted PDMS on the borders of it using a razor blade. Finally, a total of twenty-seven PDMS samples were manufactured and analysed, during three consecutive days (nine samples per day) in order to ensure a good repetitively.

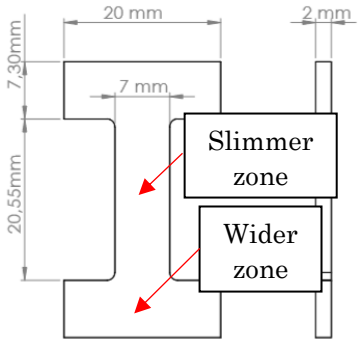

Figure 9: This illustration shows the shape and dimensions of the PDMS samples following the ASTM D412 models.

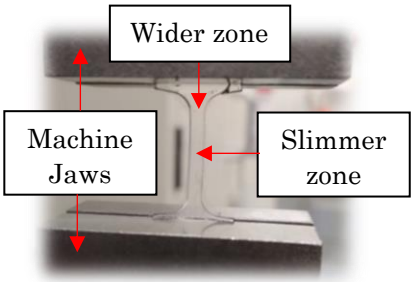

Figure 10: Schematic representation of the stress-strain tests for PDMS samples. On the top and bottom of the image the jaws of the universal testing machine can be seen, griping the PDMS sample by its wider zone, leaving ungripped only the narrow part of the sample.

The stress-strain tests for the PDMS samples were performed using the same universal testing machine and load cell used for previous peeling tests. The PDMS samples were griped by the wider zones using the machine jaws, as can be seen in **figure 10**. To perform the stress-strain tests, the upper jaw is raised up at a constant rate of 10mm/min similar to previous studies[37,8] stretching the sample, and producing a strong tension on it, until the sample collapses, obtaining the measured load needed to stretch and break the sample in front of the machine extension. The software used to record this data was NEXYGEN (see ref. page 4).

To obtain the Young modulus and the ultimate tensile stress, which magnitudes are independent of the cross-section of the samples, first we need to do a pre-treatment of the data, converting the Load (N) in front of machine extension (mm), which values are given by the software of the universal testing machine, as was commented before, to Stress σ (N/m^2) in front of Strain ε (elongation%). The Stress is obtained from dividing load needed to stretch the sample in each moment of the experiment, by the cross-sectional area of the slimmer part of the PDMS samples (for our samples 7x2mm = 14mm^2). And the strain ε is obtained from dividing the length variation of the slimmer part (ΔL) (for our samples 20.5 mm) under different amounts of stress, by its initial length (L_o). After that, we represent the Strain ε ($\Delta L/L_o$) in front of Stress σ (N/m^2), obtaining graphs like the model represented in **figure 11**. During the experiments the stress starts increasing non-linearly due to initial accommodations of the PDMS samples with the jaws, as can be seen in the initial zone of the graph. After that, an almost ideal linearly zone if found up to around 40% of the strain, like is reported on some studies[37,8]. For strains higher than 40% a non-linear behaviour is found, until the failure of the sample as can be seen in the graph on **(figure 11)**. The Young modulus was easily determined from the average slope of linearly fitted data on the linear region (for the 27 samples, no significant differences were found between the samples prepared on consecutive days). Despite of that, Young modulus studies can be performed in the non-linear zone, but more complex models must be employed[43]. The ultimate tensile stress corresponds to average value of the highest stress found before the failure of each one of the 27 samples.

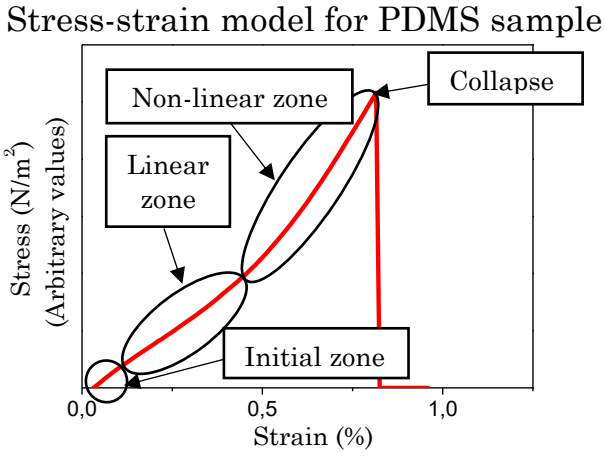

Figure 11: This graph corresponds to a model obtained from the representation of Stress in front of the strain for PDMS "dogbone" shape samples.

RESULTS AND DISCUSSION

PDMS/PDMS bond strength with partial curing

The maximum bond strength for PDMS/PDMS bonding obtained using the partial curing method, was found for the sample that was pre-cured the lowest time, as expected. In concrete obtaining a permanent bond for all the 3 samples that were pre-cured for 41 min. Since the failure of this permanent bonded sample occurred at 120 ± 10 N/m we can say that the obtained bond strength with this method is found over that value. The rest of the samples (pre-cured for 43, 45, 47 and 49 min) could be peeled-off without failure and show a decreasing average bond strength when increasing the pre-curing time (**see figure 12**), until reaching values below 20 N/m where the samples starts to be peeled extremely easy. To conclude, we should pre-cure the samples for 41 min if we want to obtain very strong bonds, nevertheless for the samples pre-cured during that time, some defects were found on the PDMS layers, due to the extremely low stiffness of the PDMS during demoulding. Then if we want to obtain high quality PDMS structures, but with still a good enough bond strength (around 51 ± 4 N/m), a pre-curing time of 43 min is more recommended. In previous studies, a maximum bond strength of 240 N/m **(see table 1)** without permanent bonding were found, but this higher recorded bond strength along with non-permanent bonding of the samples, may be due to the higher width of the samples used in this previous studies (25mm)[32], compared with ours (17mm), making them more resistant during the peeling tests. Nevertheless, the permanent bonded samples obtained with our method are strong enough for future optical-based microfluidic devices.

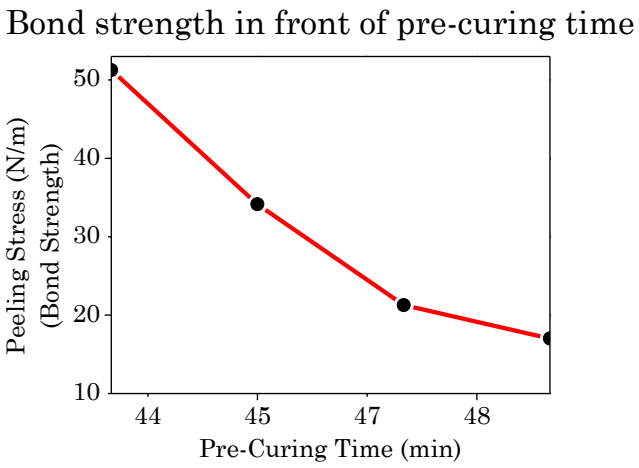

Figure 12: On this figure, the average peeling stress of the PDMS/PDMS samples bonded with partial curing time, in front of the Pre-Curing time, is shown.

PDMS/PMDS bond strength with oxygen plasma

The PDMS/PDMS samples bonded using optimized oxygen plasma conditions show an extremely irregular bond strength along the bonded interface, because the load needed to peel the sample is far away from constant during all tests. In addition, also strong average bond strength differences between samples were found **(see table 1)**, as reported in previous studies[25]. Then we can say that, the meticulously application of homogeneous pressure onto the samples, during the bonding procedure (see experimental section), allowing a homogeneous surface contact in all the bonding interface can't solve that problem. The reason of this irregular bond strength remains undetermined and needs to be studied in more detail on future studies. Despite of that, the average strength (79 ± 40 N/m, with some perma-bonds) obtained is, on average, a little bit higher than the one found for the partially cured samples during 43 min **(see table 1)**. Then to obtain high quality structures it's probably a better method. The bond strength is also slightly lower compared with previous studies[38], but we have to take in account that they used samples of 1.5mm thickness instead of 1mm, then its normal to see different results. To conclude, we can say that the nearly perma-bonded samples using the selected oxygen plasma conditions (see experimental section) are suitable for most of common microfluidic applications. Therefore, both oxygen plasma and PDMS partial curing can be used depending on the specific needs.

PDMS/glass bond strength with oxygen plasma

All the 3 sets of 3 PDMS/glass samples were bonded permanently, with a collapse point on 200 ± 5 N/mm as can be seen on **table 1**. These values are similar than the ones obtained in prior studies[44], where all samples were also perma-bonded. These results cannot be compared with the PDMS/PDMS samples results as commented in the experimental section[40]. To conclude, we can say that the bond strength obtained for PDMS/glass samples, treated under the selected plasma conditions (see experimental section), is very high, and its more than strong enough for most of the microfluidic applications.

PDMS/$KLu(WO_4)_2$ bond strength with oxygen plasma

In all the three PDMS/KLuW bonded samples, extremely low bond strength was obtained. This low bond strength was impossible to measure with the universal testing machine, because the sample is peeled-off just when is manipulated to put on the machine. Considering these results, we can say that the cleaning process may be important to perform a good bonding between PDMS and KLuW, but it's not the only important parameter. Now, our new hypothesis is that the W-O bond nature, present in the KLuW, which is different from the Si-O bond nature present in PDMS and glass, avoids the possibility to form enough active -OH groups, at least with the oxygen plasma conditions used in our experiments. Then, additional studies must be performed to test if more aggressive oxygen plasma conditions can promote the

formation of this active groups. In addition, the study of the polishing direction of the crystal may be important, because depending on it, different amounts of potentially activable oxygen atoms can be exposed to the surface of the KLuW.

Young Modulus and ultimate tensile stress of PDMS

The Young Modulus and Ultimate Tensile Stress values obtained for our PDMS Sylgard 184 was 2120 ± 58 KPa and 3110 ± 553 KPa respectively, both calculated as the average value of all the 27 samples, with a confidence interval of 0.95. The young modulus values are like some previous reported studies as can be seen on **(table 2)**. However, the Ultimate Tensile Stress of our samples is significative lower compared with previous bibliography[8]. However, its high enough for most common low-medium pressure microfluidic devices.

Table 1: On this table are summarised all the average bond strength values for PDMS/PDMS bonded samples with partial curing, including oxygen plasma treated ones, both PDMS/PDMS and PDMS/glass (permanently bonded samples are denoted by P.B). In addition, some reference values from previous studies are shown.

Pre-curing time Only for partial curing	**PDMS/PDMS** [Partial Curing]	**PDMS/PDMS** Oxygen Plasma	**PDMS/glass** Oxygen Plasma
[41 min]	>120 ± 10 N/m All P. B.	79 ± 40 N/m [3/9] P. B.	>200 ± 6 N/m All P. B.
[43 min]	51 ± 4 N/m	-	-
Previous studies			
[32]	240 N/m	-	-
[38]	-	100-200 N/m	-
[44]	-	-	All P. B.

Table 2: On the following table, the Young Modulus and Ultimate Tensile Stress results are shown, both for PDMS (Sylgard 184). Also, compared with some previous studies, where similar ASTM Models were used along with similar PDMS (Sylgard 184) preparation.

Reference	**Young Modulus (KPa)**	**Ultimate Tensile Stress (KPa)**	**Notes**
Our tests	2120 ± 58	3110 ± 553	Cured at 80°C
[37]	2125 ± (no-data)	No-data	Cured at 70°C
[8]	2050 ± 120	6250 ± 84	Cured at 100°C

CONCLUSIONS

The optimization of two direct bonding techniques like PDMS partial curing and oxygen plasma treatment were performed to bond PDMS/PDMS and PDMS/glass substrates, under certain bonding conditions, obtaining similar results to previously reported studies, where similar conditions were used. The bond strength obtained with both techniques is similar and both are suitable for most of microfluidic applications, but oxygen plasma treatment shows a slightly higher and more irregular bond strength. Still other differences between them makes one more suitable than the other to bond PDMS/PDMS surfaces in certain cases. In one hand, the low costs and low versatility of the PDMS partial curing technique compared with oxygen plasma treatment makes it more suitable for laboratories without cleanroom facilities or laboratories that wants to repeat a lot of bonding tests with similar samples. Also, the use of samples with relatively large feature size is recommended to avoid damage of very small features during demoulding of the fragile partially cured PDMS samples. In the other hand, oxygen plasma treatment can be used in a wide range of samples with different shapes, compositions and feature size, but we need to take in account that the surfaces become more hydrophilic after oxygen plasma treatment. The low bond strength obtained between PDMS/KLuW surfaces using oxygen plasma treatment, even with exhaustive cleaning process and low KLuW surface roughness, leaves the used oxygen plasma conditions as the remaining factor to be optimized, along with the polishing direction in order to obtain more accessible and easily activable oxygen atoms. The Young Modulus values are almost identical to the ones reported in previous studies where similar PDMS preparation conditions were used. However, the Ultimate Tensile Stress is half than the one previously reported. Nevertheless, these values are high enough to allow the manufacture of optical-based microfluidic devices where not extremely strong materials are required.

AKNOWLEDGEMENTS

First, I want to acknowledge Jaume Massons, for his advice, scientific guidance and personal recommendations along the master thesis. I also want to include the advices and shared knowledge transmitted with Marc Medina, Raja Anvesh and Eric Pedrol. And I appreciate too, the help and laboratory materials that Josue Mena and Nicolette Bakker provided to me for realization of the experiments in the laboratory.

REFERENCES

(1) Ren, K.; Zhou, J.; Wu, H. *Acc. Chem. Res.* **2013**, *46* (11), 2396–2406.

(2) Fujii, T. *Microelectron. Eng.* **2002**, *61–62*, 907–914.

(3) McDonald, J. C.; Whitesides, G. M. *Acc. Chem. Res.* **2002**, *35* (7), 491–499.

(4) Seethapathy, S.; Górecki, T. *Anal. Chim. Acta* **2012**, *750*, 48–62.

(5) Fernandes, A. C.; Gernaey, K. V; Krühne, U. *Biotechnol. Adv.* **2018**, 1341-1366.

(6) Mata, A.; Fleischman, A. J.; Roy, S. *Biomed. Microdevices* **2005**, *7* (4), 281–293.

(7) Friend, J.; Yeo, L. *Biomicrofluidics* **2010**, *4* (2), 1–5.

(8) Johnston, I. D.; McCluskey, D. K.; Tan, C. K. L.; Tracey, M. C. *J. Micromechanics Microengineering* **2014**, *24* (3).

(9) Wang, Z.; Volinsky, A. A.; Gallant, N. D. *J. Appl. Polym. Sci.* **2014**, *131* (22), 1–4.

(10) Choi, K. M.; Rogers, J. A. *J. Am. Chem. Soc.* **2003**, *125* (14), 4060–4061.

(11) Morent, R.; De Geyter, N.; Axisa, F.; De Smet, N.; Gengembre, L.; De Leersnyder, E.; Leys, C.; Vanfleteren, J.; Rymarczyk-Machal, M.; Schacht, E.; Payen, E. *J. Phys. D. Appl. Phys.* **2007**, *40* (23), 7392–7401.

(12) Xiong, L.; Chen, P.; Zhou, Q. *J. Adhes. Sci. Technol.* **2014**, *28* (11), 1046–1054.

(13) Félix, A. S. C.; Santiago-Alvarado, A.; Iturbide-Jiménez, F.; Licona-Morán, B. *Int. J. Eng. Sci. Innov. Technol.* **2014**, *3* (2), 563–571.

(14) Schneider, F.; Draheim, J.; Kamberger, R.; Wallrabe, U. *Sensors Actuators, A Phys.* **2009**, *151* (2), 95–99.

(15) Lee, J. N.; Park, C.; Whitesides, G. M. *Anal. Chem.* **2003**, *75* (23), 6544–6554.

(16) Eduok, U.; Faye, O.; Szpunar, J. *Prog. Org. Coatings* **2017**, *111* (May), 124–163.

(17) Gajic, M.; Lisi, F.; Kirkwood, N.; Smith, T. A.; Mulvaney, P.; Rosengarten, G. *Sol. Energy* **2017**, *150*, 30–37.

(18) Tummeltshammer, C.; Taylor, A.; Kenyon, A. J.; Papakonstantinou, I. *Opt. Lett.* **2016**, *41* (4), 713.

(19) Pérez-Calixto, D.; Zamarrón-Hernández, D.; Cruz-Ramírez, A.; Hautefeuille, M.; Hérnandez-Cordero, J.; Velázquez, V.; Grether, M. *Opt. Mater. Express* **2017**, *7* (4), 1343.

(20) Hwang, Y.; Candler, R. N. *Lab Chip* **2017**, *17* (23), 3948–3959.

(21) Chen, W.; Lam, R. H. W.; Fu, J. *Lab Chip* **2012**, *12* (2), 391–395.

(22) Hansson, J.; Hillmering, M.; Haraldsson, T.; Wijngaart, W. Van Der; Royal, K. T. H. **2015**, No. c, 563–565.

(23) Lim, S. K.; Goh, K.; Bae, T. H.; Wang, R. *Chinese J. Chem. Eng.* **2017**, *25* (11), 1653–1675.

(24) Riegger, L.; Strohmeier, O.; Faltin, B.; Zengerle, R.; Koltay, P. **2010**, *087003*, 1–6.

(25) Eddings, M. A.; Johnson, M. A.; Gale, B. K. *J. Micromechanics Microengineering* **2008**, *18* (6).

(26) Petrov, V.; Pujol, M. C.; Mateos, X.; Silvestre, Oscar; Rivier, S.; Aguiló, M.; Solé, R. M.; Liu, J.; Griebner, U.; Díaz, F. *Laser Photonics Rev.* **2007**, *1* (2), 179–212.

(27) Serres, J. M.; Loiko, P.; Mateos, X.; Yumashev, K.; Kuleshov, N.; Petrov, V.; Griebner, U.; Aguiló, M.; Díaz, F. *Opt. Mater. Express* **2015**, *5* (3), 661–667.

(28) Kuswandi, B.; Nuriman; Huskens, J.; Verboom, W. *Anal. Chim. Acta* **2007**, *601* (2), 141–155.

(29) Iliescu, C.; Taylor, H.; Avram, M.; Miao, J.; Franssila, S. *Biomicrofluidics* **2012**, *6* (1), 16505–1650516.

(30) Sasoglu, F. M.; Bohl, A. J.; Layton, B. E. *J. Micromechanics Microengineering* **2007**, *17* (3), 623–632.

(31) Lima, M. M. R. A.; Monteiro, R. C. C.; Graça, M. P. F.; Ferreira Da Silva, M. G. *J. Alloys Compd.* **2012**, *538*, 66–72.

(32) Yu, H.; Zhou, G.; Chau, F. S.; Sinha, S. K. *Microsyst. Technol.* **2011**, *17* (3), 443–449.

(33) Thompson, C. S.; Abate, A. R. *Lab Chip* **2013**, *13* (4), 632.

(34) Xiong, L.; Chen, P.; Zhou, Q. *J. Adhes. Sci. Technol.* **2014**, *28* (11), 1046–1054.

(35) Pujol, M. C.; Mateos, X.; Aznar, A.; Solans, X.; Suriach, S.; Massons, J.; Díaz, F.; Aguiló, M. *J. Appl. Crystallogr.* **2006**, *39* (2), 230–236.

(36) Bötel, F.; Zimmermann, T.; Sütel, M.; Müller, W. D.; Schwitalla, A. D. *Dent. Mater.* **2018**, 1–9.

(37) Schneider, F.; Fellner, T.; Wilde, J.; Wallrabe, U. *J. Micromechanics Microengineering* **2008**, *18* (6).

(38) Chen, C. F.; Wharton, K. *RSC Adv.* **2017**, *7* (3), 1286–1289.

(39) Cvelbar, U.; Pejovnik, S.; Mozetiè, M.; Zalar, A. *Appl. Surf. Sci.* **2003**, *210* (3–4), 255–261.

(40) Wang, Y. The effect of peeling rate and peeling angle on the peeling strength**.** Doctoral thesis**,** University of Akron**, 2014.**

(41) Liu, M.; Sun, J.; Sun, Y.; Bock, C.; Chen, Q. *J. Micromechanics Microengineering* **2009**, *19* (3).

(42) Manufacturing, C. B.; Specimens, C. R.; Determina-, T. **2009**, 1–14.

(43) Kim, T. K.; Kim, J. K.; Jeong, O. C. *Microelectron. Eng.* **2011**, *88* (8), 1982–1985.

(44) Chau, K.; Millare, B.; Lin, A.; Upadhyayula, S.; Nunez, V.; Xu, H.; Vullev, V. I. *Microfluid. Nanofluidics* **2011**, *10* (4), 907–917.